Biology of Human Tumors

Clinical Cancer Research

Clinical Implications of Phosphorylated STAT3 Expression in *De Novo* Diffuse Large B-cell Lymphoma

Chi Young Ok[1], Jiayu Chen[2], Zijun Y. Xu-Monette[1], Alexandar Tzankov[3], Ganiraju C. Manyam[4], Ling Li[1], Carlo Visco[5], Santiago Montes-Moreno[6], Karen Dybkær[7], April Chiu[8], Attilio Orazi[9], Youli Zu[10], Govind Bhagat[11], Kristy L. Richards[12], Eric D. Hsi[13], William W.L. Choi[14], J. Han van Krieken[15], Jooryung Huh[16], Xiaoying Zhao[17], Maurilio Ponzoni[18], Andrés J.M. Ferreri[18], Francesco Bertoni[19], John P. Farnen[20], Michael B. Møller[21], Miguel A. Piris[6], Jane N. Winter[22], L. Jeffrey Medeiros[1], and Ken H. Young[1]

Abstract

Purpose: Activated signal transducer and activator of transcription 3 (STAT3) regulates tumor growth, invasion, cell proliferation, angiogenesis, immune response, and survival. Data regarding expression of phosphorylated (activated) STAT3 in diffuse large B-cell lymphoma (DLBCL) and the impact of phosphorylated STAT3 (pSTAT3) on prognosis are limited.

Experimental Design: We evaluated expression of pSTAT3 in *de novo* DLBCL using immunohistochemistry, gene expression profiling (GEP), and gene set enrichment analysis (GSEA). Results were analyzed in correlation with cell-of-origin (COO), critical lymphoma biomarkers, and genetic translocations.

Results: pSTAT3 expression was observed in 16% of DLBCL and was associated with advanced stage, multiple extranodal sites of involvement, activated B-cell–like (ABC) subtype, MYC expression, and MYC/BCL2 expression. Expression of pSTAT3 predicted inferior overall survival (OS) and progression-free survival (PFS) in patients with *de novo* DLBCL. When DLBCL cases were stratified according to COO or MYC expression, pSTAT3 expression did not predict inferior outcome, respectively. Multivariate analysis showed that the prognostic predictability of pSTAT3 expression was due to its association with the ABC subtype, MYC expression, and adverse clinical features. GEP demonstrated upregulation of genes, which can potentiate function of STAT3. GSEA showed the JAK–STAT pathway to be enriched in pSTAT3$^+$ DLBCL.

Conclusions: The results of this study provide a rationale for the ongoing successful clinical trials targeting the JAK–STAT pathway in DLBCL. *Clin Cancer Res; 20(19); 5113–23. ©2014 AACR.*

Introduction

Diffuse large B-cell lymphoma (DLBCL) is the most common type of lymphoma and encompasses a heterogeneous group of tumors with several variants, subgroups, and subtypes or entities (1). With the current standard treatment of rituximab, cyclophosphamide, doxorubicin, vincristine, and prednisone (R-CHOP), 5-year overall survival (OS) for all patients with DLBCL ranges from 30% to 50% (2). Gene expression profiling (GEP) has identified distinct molecular subtypes, in particular the germinal center B-cell–like (GCB) and activated B-cell–like (ABC) DLBCL (3). The introduction of rituximab in the past decade has improved the survival of patients with DLBCL (4), but patients with ABC-like DLBCL still display a worse outcome (5).

Signal transducer and activator of transcription 3 (STAT3) is a member of the STAT family of transcription factors. In

[1]Department of Hematopathology, The University of Texas MD Anderson Cancer Center, Houston, Texas. [2]Medical School of Taizhou University, Taizhou, Zhejiang, China. [3]University Hospital, Basel, Switzerland. [4]Department of Biostatistics and Bioinformatics, The University of Texas MD Anderson Cancer Center, Houston, Texas. [5]San Bartolo Hospital, Vicenza, Italy. [6]Hospital Universitario Marques de Valdecilla, Santander, Spain. [7]Aalborg University Hospital, Aalborg, Denmark. [8]Memorial Sloan-Kettering Cancer Center, New York, New York. [9]Weill Medical College of Cornell University, New York, New York. [10]Houston Methodist Hospital, Houston, Texas. [11]Columbia University Medical Center and New York Presbyterian Hospital, New York, New York. [12]University of North Carolina School of Medicine, Chapel Hill, North Carolina. [13]Cleveland Clinic, Cleveland, Ohio. [14]University of Hong Kong Li Ka Shing Faculty of Medicine, Hong Kong, China. [15]Radboud University Nijmegen Medical Centre, Nijmegen, the Netherlands. [16]Asan Medical Center, Ulsan University College of Medicine, Seoul, Korea. [17]Zhejiang University School of Medicine, Second University Hospital, Hangzhou, China. [18]San Raffaele H. Scientific Institute, Milan, Italy. [19]IOR Institute of Oncology Research and IOSI Oncology Institute of Southern Switzerland, Bellinzona, Switzerland. [20]Gundersen Lutheran Health System, La Crosse, Wisconsin. [21]Odense University Hospital, Odense, Denmark. [22]Feinberg School of Medicine, Northwestern University, Chicago, Illinois

Note: Supplementary data for this article are available at Clinical Cancer Research Online (http://clincancerres.aacrjournals.org/).

C.Y. Ok, J. Chen, Z.Y. Xu-Monette, and K.H. Young contributed equally to this article.

Corresponding Author: Ken H. Young, Department of Hematopathology, The University of Texas MD Anderson Cancer Center, 1515 Holcombe Boulevard, Houston, TX 77030-4009. Phone: 713-745-2598; Fax: 713-792-7273; E-mail: khyoung@mdanderson.org

doi: 10.1158/1078-0432.CCR-14-0683

Translational Relevance

Activated signal transducer and activator of transcription 3 (STAT3) plays a role in tumor invasion, cell proliferation, angiogenesis, and immune response. Enhanced STAT3 activity has been found in many cancers, but its role in diffuse large B-cell lymphoma (DLBCL) has not been well studied. In this study, we showed that expression of phosphorylated STAT3 (pSTAT3) was seen in 16% of *de novo* DLBCL and was associated with advanced stage, multiple extranodal sites of involvement, activated B-cell–like (ABC) subtype, MYC expression, and MYC/BCL2 expression. Although multivariate analysis did not show expression of pSTAT3 as an independent prognostic marker, the expression of pSTAT3 showed inferior overall survival and progression-free survival in patients with *de novo* DLBCL treated with R-CHOP. pSTAT3$^+$ DLBCL upregulates genes potentiating function of STAT3, which has been found to be an attractive therapeutic target.

unstimulated cells, STAT3 is inactive and located in the cytoplasm. STAT3 is usually activated by growth factors and cytokines, such as IL6 or IL10 (6, 7). Activation of STAT3 is mediated by phosphorylation of a tyrosine residue (Tyr 705), which induces STAT3 dimerization and translocation to the nucleus (8). STAT3 transcriptional activity and DNA binding can be further modified by phosphorylation of Ser 727 (9) or p300-mediated acetylation at Lys 685 (10). Activated STAT3 regulates tumor growth, invasion, cell proliferation, angiogenesis, immune response, and survival (11, 12). Constitutive activation of STAT3 has been shown in several solid tumors, including melanoma (13) and carcinomas of the lung (14), breast (15), ovary (16), colon (17), and prostate (18), while STAT3 mutation is not a frequent event in cancers with the exception of T-cell large granular lymphocytic leukemia (19).

Both *in vitro* and *in vivo* studies have shown that STAT3 is found to be preferentially activated in the ABC DLBCL (20, 21). In some earlier studies with a limited number of patients with DLBCL treated with R-CHOP (22) or epratuzumab/R-CHOP (23), pSTAT3 expression did not show significant survival differences. However, in a very recent cohort study of patients with DLBCL treated with R-CHOP, pSTAT3 expression predicted poorer outcome (24). In this study, we evaluated the prevalence of pSTAT3 expression, its prognostic value, and potential molecular insight in a large cohort ($n = 443$) of DLBCL patients treated with R-CHOP.

Materials and Methods

Patient selection

A cohort of 443 patients with *de novo* DLBCL treated with the standard R-CHOP regimen was collected as part of The International DLBCL Rituximab-CHOP Consortium Program Study (25). All cases were centrally reviewed by a group of hematopathologists and classified according to the World Health Organization classification criteria (1). Cases that were excluded from this study included: large cell transformation of low-grade B-cell lymphoma, immunodeficiency-associated lymphoproliferative disorders (especially human immunodeficiency virus infection), primary mediastinal large B-cell lymphoma, primary cutaneous B-cell lymphoma, and primary central nervous system DLBCL. All patients had sufficient clinical and follow-up data. This study was conducted in accord with the Declaration of Helsinki. Utilization of archived diagnostic tissue samples, therapy and outcome data procurement were approved by the Institutional Review Boards (IRB) of all participating collaborative institutions. The overall study was approved by the IRB at The University of Texas MD Anderson Cancer Center (Houston, TX).

Tissue microarray immunohistochemical studies

Representative areas with the highest percentage of tumor cells were selected for tissue microarray (TMA) construction as described previously (5). Immunohistochemical (IHC) studies for various markers were performed: B-cell lymphoma 2 (BCL2), B-cell lymphoma 6 (BCL6), cyclin D1, CD10, CD30, Forkhead box protein P1 (FOXP1), GCB-expressed Transcript-1 (GCET1), multiple myeloma oncogene 1 (MUM1), MYC, nuclear factor-κB (NF-κB) components (p50, p52, p65, and c-Rel), p53, phosphorylated protein kinase B (pAKT), and phosphorylated STAT3 (pSTAT3). Receiver–operating characteristic (ROC) curves and X-tile analyses were used to assess adequate cutoff (5). When an optimal cutoff could not be determined by ROC curve and X-tile analyses, a conventional cutoff value for individual markers was decided on the basis of previous reports in the literature. The cutoff scores for these markers were as follows: 10% for cyclin D1, 20% for CD30 and p53, 30% for CD10 and BCL6, 40% for MYC, 50% for pSTAT3, 60% for GCET1, MUM1, and FOXP1, and 70% for AKT and BCL2. All markers except cyclin D1 were determined by ROC curve. Any nuclear expression of each NF-κB component was considered positive.

Fluorescence *in situ* hybridization and TP53 sequencing

Fluorescence *in situ* hybridization (FISH) analysis was performed on formalin-fixed, paraffin-embedded tissue sections using *BCL2* and *BCL6* dual-color break-apart probes (Vysis), locus-specific *IGH*/*MYC*/*CEP8* tricolor dual-fusion probes (Vysis) and a locus-specific *MYC* dual-color break-apart probe (Vysis) as reported previously (26). *TP53* exon sequencing was performed as described previously (27). Sequencing data were compared with the *TP53* reference sequence (NC_000017.10) in the Genbank database for data analysis.

GEP and gene set enrichment analysis

Total RNA was extracted from formalin-fixed, paraffin-embedded tissue samples using the HighPure RNA Extraction

Kit (Roche Applied Science) and subjected to GEP as described previously (5). The robust multiarray analysis (RMA) algorithm was used for background correction (28), and then quantile normalization was conducted (29). Cell-of-origin (COO) classification was determined primarily based on GEP data and secondarily on immunohistochemical results using the Visco-Young algorithm as described previously (5).

Gene set enrichment analysis (GSEA) was performed with GSEA application (Broad Institute at MIT, Cambridge, MA) using Kyoto Encyclopedia of Genes and Genomes (KEGG) pathway gene sets (186 gene sets). GSEA results with false discovery rate (FDR) ≤ 0.3 were considered to be significant.

Statistical analysis

Comparison among categorical variables and numerical variables was carried out by using the Fisher exact test and Kruskal–Wallis test, respectively. OS and progression-free survival (PFS) were defined from the date of diagnosis to the date of last follow-up or death and from the date of diagnosis to the date of progression or death, respectively. Survival probability was determined using the Kaplan–Meier method, with difference compared by the log-rank test. A Cox proportional-hazards model was used for univariate and multivariate analysis. All variables with $P < 0.05$ were considered to be statistically significant. SPSS Statistics V21 (IBM), GraphPad Prism V5 (GraphPad software), and X-Tile version 3.6.1 (Yale University, New Haven, CT) were used for statistical analyses.

Results

pSTAT3 expression is associated with poor outcome

The clinical features of the patient cohort are similar to that of our prior studies (30). Nuclear expression with or without cytoplasmic expression of pSTAT3 in large atypical lymphoid cells was regarded as positive in association with intensity (Supplementary Fig. S1). Expression of pSTAT3 in small, mature lymphocytes was disregarded. Clinical characteristics of patients with pSTAT3$^+$ versus pSTAT3$^-$ DLBCL are summarized in Table 1. pSTAT3 was positive in 72 (16%) patients, of which 49 were men and 23 were women. pSTAT3$^+$ DLBCL did not show distinct morphologic features compared with pSTAT3$^-$ DLBCL, having predominantly centroblastic morphology. Advanced stage (66% vs. 52%; $P = 0.036$), involvement of multiple extranodal sites (33% vs. 20%; $P = 0.026$) and the ABC subtype (67% vs. 45%; $P = 0.001$) were more commonly observed in pSTAT3$^+$ DLBCL compared with pSTAT3$^-$ DLBCL. Significant differences with respect to pSTAT3 expression were not observed for gender, age, B symptoms, Eastern Cooperative Oncology Group (ECOG) score, serum lactic dehydrogenase (LDH), International Prognostic Index (IPI), tumor size, and treatment response ($P > 0.05$).

Patients with pSTAT3$^+$ DLBCL had significantly worse OS and PFS compared with patients with pSTAT3$^-$ DLBCL (Fig. 1A and B). The 5-year OS was 48.8% for pSTAT3$^+$ DLBCL and 64.7% for patients with pSTAT3$^-$ DLBCL ($P = 0.014$). The 5-year PFS was 39.9% for pSTAT3$^+$ DLBCL and 56.2% for patients with pSTAT3$^-$ DLBCL ($P = 0.016$). The median OS was 56.9 months [95% confidence interval (CI), 18.1–95.7] for patients with pSTAT3$^+$ DLBCL and was not reached for patients with pSTAT3$^-$ DLBCL. The median PFS was 43.5 months (95% CI, 21.1–65.8) for pSTAT3$^+$ DLBCL and 78.7 months (95% CI, 61.9–95.5) for patients with pSTAT3$^-$ DLBCL.

When stratified into GCB and ABC subtypes, patients with pSTAT3$^+$ DLBCL showed a trend suggestive of inferior OS compared with patients with pSTAT3$^-$

Table 1. Clinical characteristics of 443 cases of *de novo* DLBCL with regard to pSTAT3 expression

	pSTAT3$^+$	pSTAT3$^-$	
	N (%)	*N* (%)	*P*
Patients	72 (16)	371 (84)	
Gender			
Male	49 (68)	211 (57)	
Female	23 (32)	160 (43)	0.089
Age, y			
<60	26 (36)	159 (43)	0.300
≥60	46 (64)	212 (57)	
B symptoms			
Absent	39 (60)	223 (68)	0.252
Present	26 (40)	107 (32)	
ECOG			
<2	53 (83)	267 (85)	0.706
≥2	11 (17)	48 (15)	
Stage			
I/II	24 (34)	172 (48)	0.036
III/IV	46 (66)	185 (52)	
Extranodal site			
<2	47 (67)	283 (80)	0.026
≥2	23 (33)	70 (20)	
LDH			
Normal	25 (37)	116 (35)	0.780
Elevated	42 (63)	216 (65)	
IPI			
0–2	32 (44)	210 (58)	0.051
3–5	40 (56)	154 (42)	
Tumor size, cm			
<6	34 (63)	194 (68)	0.529
≥6	20 (37)	92 (32)	
Treatment response			
CR/PR	63 (88)	332 (90)	0.678
No response	9 (12)	39 (10)	
COO classification			
GCB	24 (33)	204 (55)	0.001
ABC	48 (67)	166 (45)	

Abbreviations: CR, complete remission; PR, partial remission.

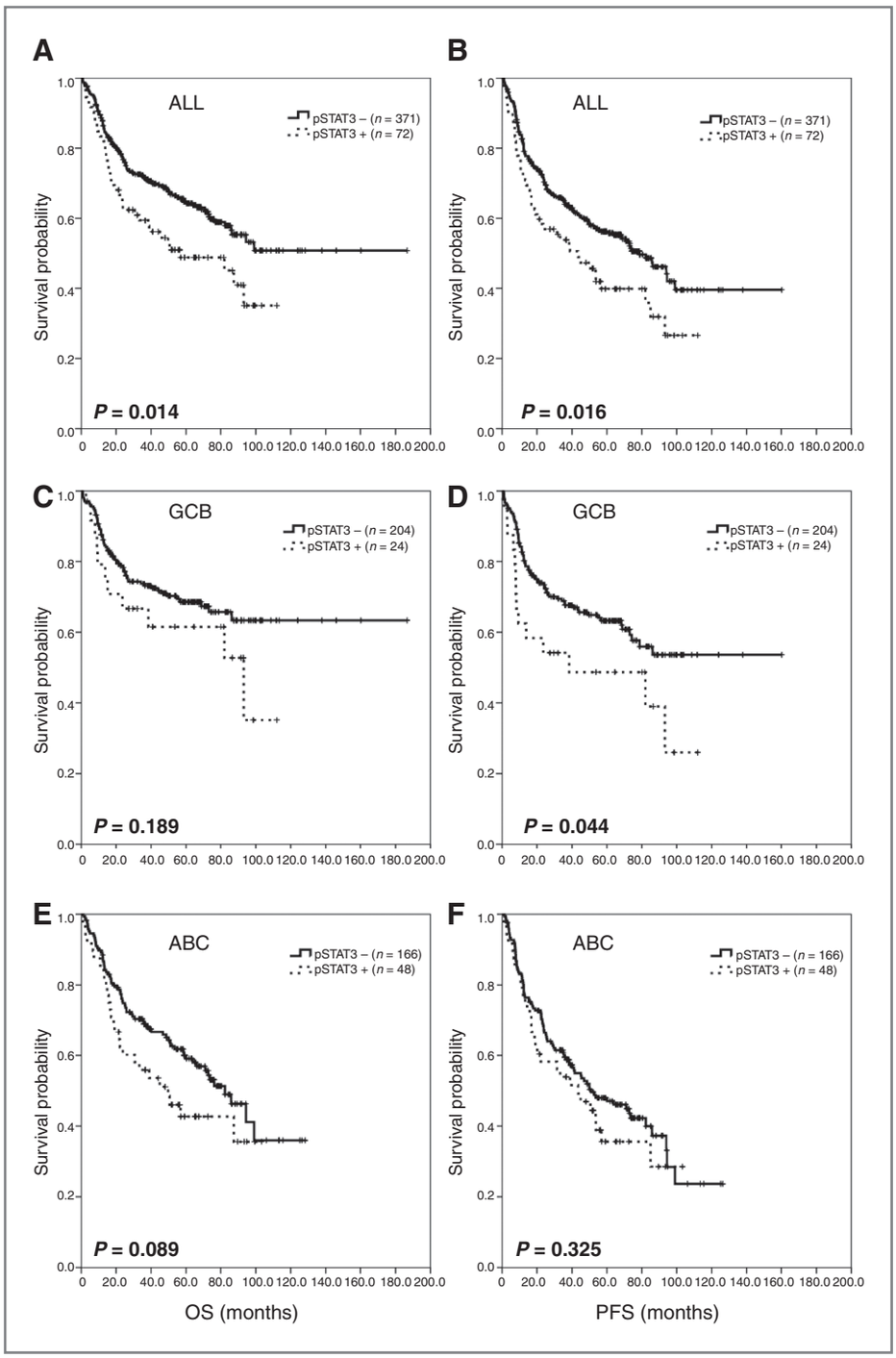

Figure 1. Survival impact of pSTAT3 in *de novo* DLBCL. A and B, overall, pSTAT3 showed inferior OS and PFS. C and D, in the GCB subtype, significant survival difference is only seen in PFS ($P = 0.044$). E and F, in the ABC subtype, significant survival difference is not seen in either OS or PFS.

DLBCL in the GCB subgroup ($P = 0.189$) and the ABC subgroup ($P = 0.089$), respectively (Fig. 1C and E). Patients with pSTAT3$^+$ DLBCL had worse PFS in the GCB subgroup ($P = 0.044$), but showed no significant difference of survival in the ABC subgroup ($P = 0.325$; Fig. 1D and F). Separating stage I–II vs. III–IV, pSTAT3 retained prognostic value in the lower stage subgroup ($P = 0.008$ for OS and $P = 0.021$ for PFS), but not in the advanced-stage subgroup ($P = 0.591$ for OS and $P = 0.441$ for PFS). In the patient subgroup with less than two extranodal sites of involvement, pSTAT3 predicted poorer prognosis ($P = 0.029$ for OS and $P = 0.028$ for PFS), but not in patients with two or more extranodal sites ($P = 0.958$ for OS and $P = 0.881$ for PFS, Supplemental Table S6).

We also measured *STAT3* mRNA levels and evaluated whether *STAT3* mRNA level correlated with pSTAT3 expression. To measure mRNA expression of the *STAT3* gene, from the GEP dataset, we retrieved the intensity of four STAT3 probe-sets and used the average value as *STAT3* expression at the mRNA level. Patients were divided into three groups for survival analysis according to the mean values of mRNA expression: low *STAT3* mRNA (< mean − one standard deviation), high *STAT3* mRNA (> mean + 1 standard deviation), and intermediate *STAT3* mRNA levels (the remaining cases). The mean values of pSTAT3 expression in cases with low, intermediate, and high *STAT3* mRNA were 12%, 22%, and 36%, respectively, showing correlation between STAT3 mRNA and pSTAT3 expression ($P = 0.0002$; Supplementary Fig. S2). However, *STAT3* mRNA did not show significant difference with respect to OS in all cases ($P = 0.1487$) and ABC DLBCL ($P = 0.6183$). Although significant stratification was seen in GCB DLBCL, cases with high *STAT3* mRNA and low mRNA showed the best and worst survival, respectively. Seven cases with high *STAT3* mRNA in GCB DLBCL is insufficient number to achieve statistical power and could be an random event. The worse prognosis in cases with low *STAT3* mRNA could be due to contamination from background inflammatory cells.

pSTAT3 expression is associated with MYC and MYC/BCL2 expression

Immunohistochemical and genetic characteristics of $pSTAT3^+$ and $pSTAT3^-$ DLBCL are summarized in Table 2. An association between STAT3 and the *MYC* and *BCL2* genes has been reported previously by other investigators in limited patient series (31, 32). Therefore, in this study, we comprehensively assessed MYC and BCL2 expression with respect to pSTAT3, in association with genetic aberrations. MYC and MYC/BCL2 double expression were more commonly observed in $pSTAT3^+$ DLBCL cases ($P < 0.001$ and $P = 0.001$, respectively). However, BCL2 expression was not significantly different in DLBCL cases positive or negative for pSTAT3 expression ($P = 0.420$). Rearrangements of *BCL2*, *BCL6*, or *MYC* detected by FISH did not show any significant differences between $pSTAT3^+$ DLBCL and $pSTAT3^-$ DLBCL ($P > 0.05$). One $pSTAT3^+$ case (2%) showed rearrangements of both *MYC* and *BCL6* genes, and no case had coexistent *MYC* and *BCL2* rearrangements. Regarding *TP53* exon mutations detected by sequencing, *TP53* gene deletions detected by

Table 2. Immunophenotypic and genetic characteristics of 433 cases of *de novo* DLBCL with regard to pSTAT3 expression

	Overall (%)	$pSTAT3^+$ (%)	$pSTAT3^-$ (%)	*P*
MYC expression	260/398 (65)	61/65 (94)	199/333 (60)	<0.001
BCL2 expression	192/398 (48)	35/66 (53)	157/332(47)	0.420
MYC/BCL2 coexpression	130/396 (33)	34/65 (52)	96/331 (29)	0.001
BCL2 rearranged	69/378 (18)	7/59 (12)	62/319 (19)	0.201
BCL6 rearranged	107/321 (33)	20/50 (40)	87/271 (32)	0.327
MYC rearranged	35/382 (9)	4/62 (6)	31/320 (10)	0.630
Double hit[a]	13/287 (5)	1/42 (2)	12/245 (5)	0.700
TP53 deletion	47/402 (12)	5/67 (7)	42/335 (13)	0.300
TP53 mutated	91/408 (22)	13/67 (19)	78/341 (23)	0.631
p53 expression	140/395 (36)	27/66 (41)	113/329 (34)	0.326
p50 expression	154/428 (36)	27/70 (39)	127/358 (35)	0.683
p52 expression	119/422 (28)	27/71 (38)	92/351 (26)	0.050
p65 expression	144/428 (34)	27/71 (38)	117/357 (33)	0.411
cRel expression	99/422 (24)	13/67 (19)	86/355 (24)	0.436
p50/p65 coexpression	77/422 (18)	14/70 (20)	63/352 (18)	0.735
p50/cRel coexpression	47/420 (11)	6/67 (9)	41/353 (12)	0.674
p52/p65 coexpression	41/414 (10)	11/70 (16)	30/344 (9)	0.081
p52/cRel coexpression	44/406 (11)	6/66 (9)	38/340 (11)	0.829
Classical NF-κB expression	100/427 (23)	15/70 (21)	85/357 (24)	0.758
Alternative NF-κB expression	71/417 (17)	12/70 (17)	59/347 (17)	1.000
NF-κB expression[b]	134/417 (32)	20/69 (29)	114/348 (33)	0.575
CD30 expression	72/439 (16)	12/72 (17)	60/367 (16)	1.000
pAKT expression	76/435 (17)	17/71 (24)	59/364 (16)	0.125
Cyclin D1 expression	10/432 (2)	2/71 (3)	8/361 (2)	0.672

[a]Double hit, *MYC* and *BCL2* or *BCL6* rearrangements.

[b]Summation of the classical and alternative NF-κB pathway expression.

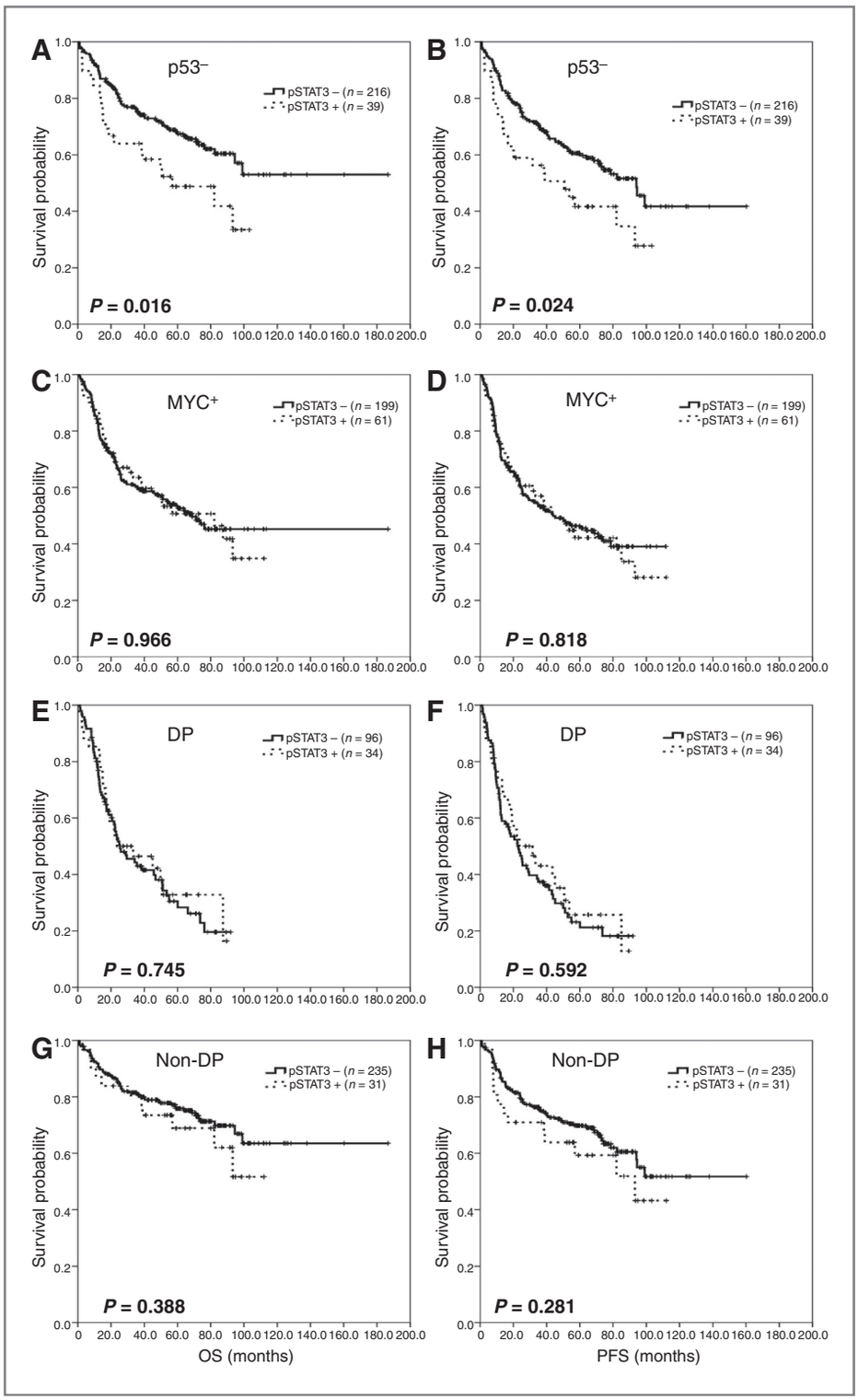

Figure 2. Survival impact of pSTAT3 in subsets of *de novo* DLBCL. A and B, in group of DLBCL without p53 expression by immunohistochemistry, pSTAT3 expression shows adverse effect in OS and PFS. C and D, in the group of MYC expression, pSTAT3 expression does not show different outcome in OS and PFS. E and F, in the group of MYC/BCL2 double protein expression (DP), pSTAT3 expression does not have prognostic impact. G and H, in the group without MYC/BCL2 double expression (non-DP), pSTAT3 expression does not show differences in OS and PFS.

FISH, or p53 expression, there were no significant differences between pSTAT3$^+$ and pSTAT3$^-$ DLBCL cases ($P > 0.05$). Stratifying our cohort according to p53 expression, pSTAT3$^+$ DLBCL showed a significant worse outcome in OS ($P = 0.016$) and PFS ($P = 0.024$) in the p53-negative group (Fig. 2A and B). A total of 13 (19%) DLBCLs harbored *TP53* mutations. All of the *TP53* mutations were confined to exons 4 to 8, which are the most critical sites

for DNA binding (33). Eleven cases were missense mutations and two cases were nonsense mutations.

Association of pSTAT3 expression with NF-κB components, cyclin D1 or pAKT

Cooperation of STAT3 and NF-κB is well known (21, 34). However, few studies have correlated expression of individual NF-κB components (p50, p52, p65, and cRel) with pSTAT3 expression. In this study, a significant trend that p52 single component and p52/p65 dimer were more commonly observed in pSTAT3$^+$ DLBCL compared with pSTAT3$^-$ DLBCL ($P = 0.05$ and 0.081, respectively). Other NF-κB single components or combinations of NF-κB dimers (p50/p65, p50/cRel, and p52/cRel) were not more commonly expressed in pSTAT3$^+$ DLBCL ($P > 0.05$). Neither the classical NF-κB pathway (p50/p65 or p50/cRel), nor the alternative NF-κB pathway (p52/p65 or p52/cRel), nor both showed significant association with pSTAT3 expression ($P > 0.05$).

Cyclin D1 is a known downstream target of pSTAT3 (35) and protein kinase B (AKT) can be activated via the JAK–STAT pathway (36). Therefore, we assessed protein expression of cyclin D1 and pAKT in this study. Neither cyclin D1 nor pAKT protein expression was significantly different between pSTAT3$^+$ DLBCL and pSTAT3$^-$ DLBCL ($P > 0.05$).

Multivariate analysis of prognostic parameters

Stratified according to MYC expression, the prognostic effect of pSTAT3 was abrogated in patients with MYC$^+$ DLBCL ($P = 0.966$ for OS and $P = 0.818$ for PFS; Fig. 2C and D). Survival analysis was not performed in MYC$^-$ group because only 4 MYC$^-$/pSTAT3$^+$ cases were present. Stratifying DLBCL cases into MYC/BCL2 protein double-positive (DP) and non–double-positive (non-DP) groups, pSTAT3 showed no effect on survival in the DP ($P = 0.745$ for OS and $P = 0.592$ for PFS) as well as the non-DP patient subgroups ($P = 0.388$ for OS and $P = 0.281$ for PFS; Fig. 2E–H). When stratifying DP and non-DP subgroups into COO classification, no effect on survival was seen (Supplementary Fig. S3 and Supplementary Table S1).

Univariate analysis identified advanced age, multiple extranodal sites of involvement, ABC subtype, pSTAT3 expression, and MYC expression increased hazard in patients with *de novo* DLBCL ($P < 0.05$ in all variables). Multivariate analysis using these five variables demonstrated that pSTAT3 is not an independent variable ($P = 0.460$ for OS and $P = 0.523$ for PFS). All the other variables were significant (Table 3).

GEP and GSEA of pSTAT3$^+$ DLBCL

To further characterize pSTAT3$^+$ DLBCL, we compared the GEP signatures of pSTAT3$^+$ and pSTAT3$^-$ DLBCL using the Affymetrix HGU133plus2 platform (Affymetrix; Fig. 3A). With a FDR threshold of 0.3, a total of 26 genes were differentially expressed between the two groups, including 15 upregulated genes and 11 downregulated genes in pSTAT3$^+$ DLBCL. Among the upregulated genes in pSTAT3$^+$ DLBCL, *STAT3*, *IL2RA*, *CD44*, *EPHA4*, and *CDK5R1* were significant. Upregulation of the *IL2RA* gene suggests a positive feedback mechanism of pSTAT3 because IL2 activates STAT3 via activating Janus-activated kinase (JAK). CD44 can acetylate and dimerize STAT3 in a growth factor- and cytokine-independent manner and has been shown to be involved in cell migration, tumor invasion, and metastasis, potentiating STAT3 function and partially explaining the adverse outcome in pSTAT3$^+$ DLBCL (37). *EPHA4* encodes ephrin receptor A4, which has receptor tyrosine kinase activity. *CDK5R1* encodes CDK5/p35, which is a downstream target molecule of ephrin receptor A4 and its expression has been shown to predict inferior survival in patients with non–small cell lung cancer (38). Many of the downregulated genes encode proteins of unknown function. Huang and colleagues (24) proposed a prognostically valuable 11-gene signature in PY-STAT3$^+$ DLBCLs. The 11 genes were *HSD17B4*, *MT1X*, *NAT8L*, *PCNX*, *RHEB*, *RNF149*, *SLA*, *SLC2A13*, *ZNF805*, *C15orf29*, and *ZNF420*. However, few of these genes (*RHEB*, *PCNX*, and *ZNF420*) were expressed with marginal significance for survival in our cohort and combination of the 11 genes showed overall significant trend ($P = 0.07$). GSEA analysis showed trends for several gene sets, including the JAK–STAT pathway gene set, being enriched in pSTAT3$^+$ DLBCL (Fig. 3B).

Discussion

In this study, 16% of *de novo* DLBCL cases expressed pSTAT3. The prevalence of pSTAT3 expression in DLBCL is lower than that reported in earlier studies, in which 30%

Table 3. Multivariate analysis of clinicopathologic variables in *de novo* DLBCL

	OS		PFS	
	HR (95% CI)	*P*	HR (95% CI)	*P*
Stage III/IV	2.182 (1.464–3.252)	<0.001	1.758 (1.235–2.503)	0.002
EN sites ≥2	1.560 (1.066–2.284)	0.022	1.662 (1.161–2.379)	0.005
ABC subtype	1.473 (1.050–2.067)	0.025	1.483 (1.086–2.026)	0.013
pSTAT3	0.856 (0.568–1.292)	0.460	0.882 (0.601–1.295)	0.523
MYC	2.188 (1.440–3.326)	<0.001	1.971 (1.359–2.860)	<0.001

Abbreviation: EN sites, extranodal sites.

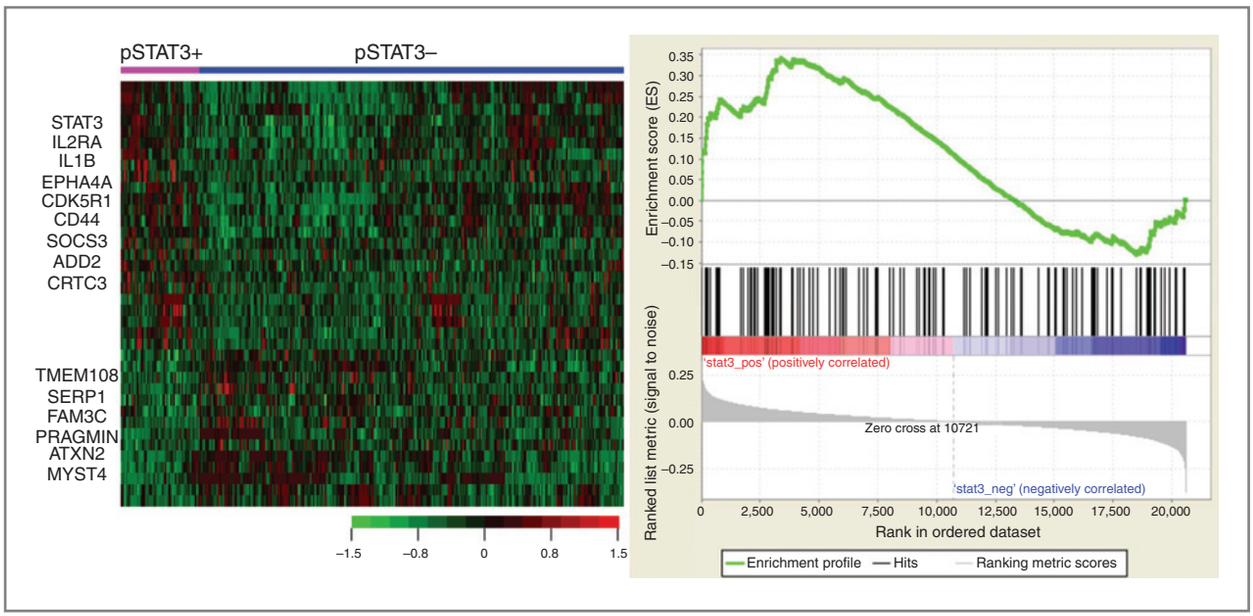

Figure 3. GEP and GSEA. A, GEP shows that pSTAT3$^+$ DLBCL is genetically distinct from pSTAT3$^-$ DLBCL. Representative upregulated and downregulated genes in the pSTAT3$^+$ DLBCL are illustrated at the upper end and lower end, respectively. B, GSEA shows a trend that the KEGG JAK–STAT pathway is enriched in the pSTAT3$^+$ DLBCL.

to 40% of DLBCL expressed pSTAT3 (22, 24, 39, 40). Of note, pSTAT3 expression are 67%, 51%, 34%, 23%, 16%, and 11% if the pSTAT3 cutoffs are 10%, 20%, 30%, 40%, 50%, and 60%, respectively (Supplementary Table S2). With 30% cutoff, the prevalence of pSTAT3 expression is in similar range to prior data. However, our cutoff value for pSTAT3 was determined on the basis of a ROC curve to achieve optimal sensitivity and specificity. Compared with survival analysis using 50% cutoff (Fig. 1), 30% cutoff does not show any significant differences between pSTAT3$^+$ DLBCL and pSTAT3$^-$ DLBCL (Supplementary Fig. S4). Furthermore, no clinical differences are observed between the two groups using 30% cutoff except COO classification (Supplementary Table S3). We additionally conducted survival analysis in four separate quartile groups (Q1: <30%; Q2: ≥30% and <50%; Q3: ≥50% and <70%; and Q4: ≥70%; Supplementary Table S4). Although overall quartile analysis showed significant stratification, Q3 and Q4 did not show significant difference (Supplementary Fig. S5, bottom row). Merging Q3 and Q4, we conducted survival analysis in three groups (T1: <30%; T2: ≥30% and <50%; and T3: ≥50%; Supplementary Table S5). T2 and T3 showed significant difference, whereas T1 and T2 did not (Supplementary Fig. S5, top row). On the basis of our analysis, we chose 50% as an optimal cutoff for pSTAT3 expression. With 50% cutoff, we could minimize possible contamination of pSTAT3 expression in non-lymphoma cells. As has also been shown by others (22–24, 39), pSTAT3 was more commonly expressed in ABC-DLBCL. Such a finding can be explained by Ding and colleagues (20) who showed that *STAT3* gene transcription was negatively regulated by BCL6, hence providing a basis for STAT3 activation in ABC-DLBCL. We also showed that *STAT3* mRNA level is quantitatively correlated with pSTAT3 expression. (Supplementary Fig. S2)

We showed that pSTAT3 expression in *de novo* DLBCL is associated with adverse outcome, confirming a similar observation by Huang and colleagues and Meier and colleagues (24, 40). We could not, however, show that pSTAT3 expression is an independent prognostic factor in patients with DLBCL in multivariate analysis (Table 3). Furthermore, pSTAT3 expression is associated with MYC expression and MYC/BCL2 double expression. However, when MYC expression was controlled, pSTAT3 did not significantly predict prognosis (Fig. 2). In cases with MYC/BCL2 DP or non-DP, significant difference was not observed, either. No survival difference was seen after stratified into GCB/ABC in DP and non-DP groups (Supplementary Fig. S4). Furthermore, multivariate analysis did not identify pSTAT3 as an independent hazard. Instead, other variables, such as stage, COO classification, and MYC expression, were shown to be independent prognosticators (Table 3). We additionally conducted bivariate analyses including each variable in the multivariate analysis and pSTAT3 expression to see if increased hazardous effect of pSTAT3 is observed (Supplementary Table S6). pSTAT3 did not show increased hazard except when pSTAT3 coanalyzed with ABC phenotype. Therefore, inferior outcome of patients with pSTAT3$^+$ DLBCL appeared to be a result of the associated poor prognostic indicators such as advanced-stage disease and multiple extranodal sites of involvement. Interestingly, in patients with less aggressive or advanced disease, such as limited stage (stage I or II), involvement of less than 2 extranodal sites, absence of p53 expression, or GCB-type

DLBCL, pSTAT3 expression showed a worse outcome. Our data therefore suggest that pSTAT3 expression predicts poor outcome in less aggressive/advanced DLBCL, but it does not provide additional survival impact in patients with advanced disease or with already known poor prognostic factors, including MYC expression or BCL2/MYC coexpression (23, 30, 41).

The results of GEP analysis in this study showed that pSTAT3$^+$ DLBCL is distinct from pSTAT3$^-$ DLBCL. Many of the upregulated genes, such as *STAT3*, *IL2RA*, *IL1B*, *EPHA4*, and *CDK5R1* in pSTAT3$^+$ DLBCL contain several binding sites for STAT3 in their promoters and some of the upregulated genes have been reported to correlate with aggressive features in carcinomas (37, 38). The results of GSEA also provide evidence that the JAK–STAT pathway is enriched in pSTAT3$^+$ DLBCL, although the statistical significance is marginal. In a recent study by Huang and colleagues (24), the authors suggested that an 11-gene signature was associated with poor OS in patients with STAT3$^+$ DLBCL, treated with CHOP and R-CHOP, respectively, without achieving statistical significance. Some of these genes were marginally upregulated in pSTAT3$^+$ DLBCL by GEP in our study, partially in agreement with Huang and colleagues (24).

Although our GEP results did not show that *MYC* was significantly upregulated in pSTAT3$^+$ DLBCL, it is not surprising to observe the correlation between MYC expression and pSTAT3 in this study because *MYC* is a known target of STAT3 (31, 42, 43). Kikuchi and colleagues (31) demonstrated that STAT3 was essential for *MYC* mRNA expression in a proB cell line (BAF/B03). Barre and colleagues (42) showed that STAT3 was recruited to the *MYC* promoters upon IL6 stimulation of glioblastoma cells using chromatin immunoprecipitation (ChIP). Bowman and colleagues (43) reported that MYC expression was induced by STAT3 in fibroblasts. In primary DLBCL patient samples, Gupta and colleagues (23) showed a trend between pSTAT3 and MYC expression in a small study of 23 patients.

NF-κB and pSTAT3 are known to cooperate and four different modes of reciprocal interaction in transcriptional control have been suggested (34). (i) STAT3/p65 in the nucleus can recruit p300 histone acetyltransferase, which acetylates histone as well as p65. Acetylated p65 is less prone to nuclear export, hence persists longer in the nucleus where it is transcriptionally active. (ii) In the nucleus, NF-κB/STAT3 can bind to particular DNA target sequences at sites where neither can bind alone. (iii) Unphosphorylated STAT3 can bind with and displace IκB so that NF-κB can be activated without any upstream signals. (iv) I-κBζ, which is induced by NF-κB, can bind to STAT3 and inhibit STAT3-DNA binding. We showed a significant trend that p52 single expression and p52/p65 dimer expression were more commonly seen in pSTAT3$^+$ DLBCL, supporting a cross-talk between STAT3 and NF-κB (44, 45). Lam and colleagues (21) showed the induction of IL6 and IL10 by the NF-κB pathway in ABC DLBCL cell lines. Considering constitutive activation of NF-κB and common pSTAT3 expression in ABC DLBCL, targeting either or both of them appears to be an attractive addition to the current R-CHOP regimen especially in this subtype.

Recently, STAT3 was found to be a substrate of histone deacetylase 3 (HDAC3) in ABC-DLBCL (46). Although the primary substrates of HDACs are histones, nonhistone proteins, including NF-κB transcription factors, could also be targeted by HDACs (47). In the context of cross-talk between NF-κB and STAT3, targeting HDAC seems to be a reasonable approach. Gupta and colleagues (46) demonstrated that a HDAC inhibitor panobinostat (also known as LBH589) could dephosphorylate STAT3 in an ABC-DLBCL cell line, (Ly3), as well as DLBCL patient samples, in a dose-dependent manner. However, a recent phase I study using panobinostat with everolimus in patients with relapsed and refractory lymphoma did not show a response in patients with DLBCL (48). Lam and colleagues (21) also showed that blocking JAK/STAT3 activation using a JAK inhibitor in ABC-DLBCL cell lines reduces cell proliferation and survival. They also demonstrated a synergistic effect on tumor cell death by combining JAK/STAT3 and NF-κB inactivation in ABC-DLBCL cell lines. A phase II clinical trial using an oral JAK inhibitor (INCB18424) is in progress in patients with relapsed or refractory DLBCL or peripheral T-cell lymphoma (NCT01431209).

Scuto and colleagues (49) demonstrated that inhibition of STAT3 with short hairpin RNA was associated with apoptosis in a human ABC-like DLBCL cell line (Ly3), as well as tumor regression in nonobese diabetic/severe combined immunodeficient (NOD/SCID) mice injected by Ly3 cells. In their study, direct STAT3 inhibition induced significant reduction of STAT3 targets such as MYC and survivin at the protein level. Survivin is an antiapoptotic protein and has been shown to be unfavorable prognostic marker in DLBCL (50). Furthermore, Scuto and colleagues also showed that inhibition of STAT3 thwarted IL10-dependent STAT3 activation, proving that STAT3 can be an attractive therapeutic target. Currently, a multi-institution phase I/II clinical trial using an antisense oligonucleotide inhibitor targeting STAT3 in patients with DLBCL is in progress (NCT01563302).

In summary, pSTAT3 expression is more commonly seen in ABC-DLBCL and is associated with advanced-stage, multiple extranodal sites of involvement, MYC expression, and MYC/BCL2 double expression. Although pSTAT3 is not an independent prognostic marker, pSTAT3 expression in DLBCL predicts an unfavorable outcome. GEP suggests that pSTAT3$^+$ DLBCL is molecularly distinct from pSTAT3$^-$ DLBCL with a unique oncogenic pathway activation signature, which identify a group of patients who might benefit from the use of molecularly targeted therapies. Ongoing successful clinical trials targeting the STAT3 pathway may shed new light on the significance of STAT3 expression, particularly in refractory/resistant DLBCL.

Disclosure of Potential Conflicts of Interest

No potential conflicts of interest were disclosed.

Authors' Contributions

Conception and design: C.Y. Ok, Z.Y. Xu-Monette, J.H. van Krieken, K.H. Young
Development of methodology: J. Chen, Z.Y. Xu-Monette, K.H. Young
Acquisition of data (provided animals, acquired and managed patients, provided facilities, etc.): C.Y. Ok, J. Chen, Z.Y. Xu-Monette, A. Tzankov, C. Visco, S. Montes-Moreno, K. Dybkær, A. Chiu, A. Orazi, Y. Zu, G. Bhagat, K.L. Richards, E.D. Hsi, W.W.L. Choi, J.H. van Krieken, J. Huh, X. Zhao, M. Ponzoni, A.J.M. Ferreri, J.P. Farnen, M.B. Møller, M.A. Piris, J.N. Winter, K.H. Young
Analysis and interpretation of data (e.g., statistical analysis, biostatistics, computational analysis): C.Y. Ok, J. Chen, Z.Y. Xu-Monette, A. Tzankov, G.C. Manyam, L. Li, C. Visco, W.W.L. Choi, X. Zhao, M.B. Møller, L.J. Medeiros, K.H. Young
Writing, review, and/or revision of the manuscript: C.Y. Ok, J. Chen, Z.Y. Xu-Monette, A. Tzankov, L. Li, K. Dybkær, A. Chiu, A. Orazi, G. Bhagat, K.L. Richards, E.D. Hsi, J.H. van Krieken, X. Zhao, M. Ponzoni, F. Bertoni, M.B. Møller, M.A. Piris, J.N. Winter, L.J. Medeiros, K.H. Young
Administrative, technical, or material support (i.e., reporting or organizing data, constructing databases): C.Y. Ok, J. Chen, L. Li, A. Chiu, Y. Zu, A.J.M. Ferreri, M.B. Møller, L.J. Medeiros, K.H. Young
Study supervision: K.H. Young
Other (provision of case material and clinical data): A. Orazi
Other (approval of final article): A.J.M. Ferreri

Grant Support

This work was supported by the Fellowship Award (to C.Y. Ok); the Harold C. and Mary L. Daily Endowment Fellowships and Shannon Timmins Fellowship for Leukemia Research Award (to Z.Y. Xu-Monette); The University of Texas MD Anderson Cancer Center Institutional Research Grant Award, an MD Anderson Lymphoma Specialized Programs of Research Excellence (SPORE) Research Development Program Award, an MD Anderson Myeloma SPORE Research Development Program Award, MD Anderson Collaborative Research Funds with High-Throughput Molecular Diagnostics, Gilead Pharmaceutical, Adaptive Biotechnologies, and Roche Molecular Systems (to K.H. Young). This work was also partially supported by National Cancer Institute and NIH grants (R01CA138688, 1RC1CA146299, P50CA136411, and P50CA142509), and by the MD Anderson Cancer Center Support Grant CA016672.

The costs of publication of this article were defrayed in part by the payment of page charges. This article must therefore be hereby marked *advertisement* in accordance with 18 U.S.C. Section 1734 solely to indicate this fact.

Received March 20, 2014; revised June 11, 2014; accepted July 18, 2014; published OnlineFirst August 14, 2014.

References

1. Stein H, Warnke RA, Chan WC, Jaffe ES, Chan JKC, Gatter KC, et al. editors. Diffuse large B-cell lymphoma, not otherwise specified. 4th ed. Lyon, France: International Agency for Research on Cancer (IARC); 2008.
2. Cultrera JL, Dalia SM. Diffuse large B-cell lymphoma: current strategies and future directions. Cancer Control 2012;19:204–13.
3. Alizadeh AA, Eisen MB, Davis RE, Ma C, Lossos IS, Rosenwald A, et al. Distinct types of diffuse large B-cell lymphoma identified by gene expression profiling. Nature 2000;403:503–11.
4. Sehn LH, Donaldson J, Chhanabhai M, Fitzgerald C, Gill K, Klasa R, et al. Introduction of combined CHOP plus rituximab therapy dramatically improved outcome of diffuse large B-cell lymphoma in British Columbia. J Clin Oncol 2005;23:5027–33.
5. Visco C, Li Y, Xu-Monette ZY, Miranda RN, Green TM, Tzankov A, et al. Comprehensive gene expression profiling and immunohistochemical studies support application of immunophenotypic algorithm for molecular subtype classification in diffuse large B-cell lymphoma: a report from the International DLBCL Rituximab-CHOP Consortium Program Study. Leukemia 2012;26:2103–13.
6. Niemand C, Nimmesgern A, Haan S, Fischer P, Schaper F, Rossaint R, et al. Activation of STAT3 by IL-6 and IL-10 in primary human macrophages is differentially modulated by suppressor of cytokine signaling 3. J Immunol 2003;170:3263–72.
7. Yu H, Jove R. The STATs of cancer—new molecular targets come of age. Nat Rev Cancer 2004;4:97–105.
8. Bhattacharya S, Schindler C. Regulation of Stat3 nuclear export. J Clin Invest 2003;111:553–9.
9. Wen Z, Zhong Z, Darnell JE Jr. Maximal activation of transcription by Stat1 and Stat3 requires both tyrosine and serine phosphorylation. Cell 1995;82:241–50.
10. Wang R, Cherukuri P, Luo J. Activation of Stat3 sequence-specific DNA binding and transcription by p300/CREB-binding protein-mediated acetylation. J Biol Chem 2005;280:11528–34.
11. Bromberg JF, Wrzeszczynska MH, Devgan G, Zhao Y, Pestell RG, Albanese C, et al. Stat3 as an oncogene. Cell 1999;98:295–303.
12. Calo V, Migliavacca M, Bazan V, Macaluso M, Buscemi M, Gebbia N, et al. STAT proteins: from normal control of cellular events to tumorigenesis. J Cell Physiol 2003;197:157–68.
13. Xie TX, Huang FJ, Aldape KD, Kang SH, Liu M, Gershenwald JE, et al. Activation of stat3 in human melanoma promotes brain metastasis. Cancer Res 2006;66:3188–96.
14. Gao SP, Mark KG, Leslie K, Pao W, Motoi N, Gerald WL, et al. Mutations in the EGFR kinase domain mediate STAT3 activation via IL-6 production in human lung adenocarcinomas. J Clin Invest 2007;117:3846–56.
15. Berishaj M, Gao SP, Ahmed S, Leslie K, Al-Ahmadie H, Gerald WL, et al. Stat3 is tyrosine-phosphorylated through the interleukin-6/glycoprotein 130/Janus kinase pathway in breast cancer. Breast Cancer Res 2007;9:R32.
16. Yang C, Lee H, Jove V, Deng J, Zhang W, Liu X, et al. Prognostic significance of B-cells and pSTAT3 in patients with ovarian cancer. PLoS ONE 2013;8:e54029.
17. Lin L, Liu A, Peng Z, Lin HJ, Li PK, Li C, et al. STAT3 is necessary for proliferation and survival in colon cancer-initiating cells. Cancer Res 2011;71:7226–37.
18. Barton BE, Murphy TF, Shu P, Huang HF, Meyenhofer M, Barton A. Novel single-stranded oligonucleotides that inhibit signal transducer and activator of transcription 3 induce apoptosis *in vitro* and *in vivo* in prostate cancer cell lines. Mol Cancer Ther 2004;3:1183–91.
19. Koskela HL, Eldfors S, Ellonen P, van Adrichem AJ, Kuusanmaki H, Andersson EI, et al. Somatic STAT3 mutations in large granular lymphocytic leukemia. N Engl J Med 2012;366:1905–13.
20. Ding BB, Yu JJ, Yu RY, Mendez LM, Shaknovich R, Zhang Y, et al. Constitutively activated STAT3 promotes cell proliferation and survival in the activated B-cell subtype of diffuse large B-cell lymphomas. Blood 2008;111:1515–23.
21. Lam LT, Wright G, Davis RE, Lenz G, Farinha P, Dang L, et al. Cooperative signaling through the signal transducer and activator of transcription 3 and nuclear factor-{kappa}B pathways in subtypes of diffuse large B-cell lymphoma. Blood 2008;111:3701–13.
22. Wu ZL, Song YQ, Shi YF, Zhu J. High nuclear expression of STAT3 is associated with unfavorable prognosis in diffuse large B-cell lymphoma. J Hematol Oncol 2011;4:31.
23. Gupta M, Maurer MJ, Wellik LE, Law ME, Han JJ, Ozsan N, et al. Expression of Myc, but not pSTAT3, is an adverse prognostic factor for diffuse large B-cell lymphoma treated with epratuzumab/R-CHOP. Blood 2012;120:4400–6.
24. Huang X, Meng B, Iqbal J, Ding BB, Perry AM, Cao W, et al. Activation of the STAT3 signaling pathway is associated with poor survival in diffuse large B-cell lymphoma treated with R-CHOP. J Clin Oncol 2013;31:4520–8.
25. Xu-Monette ZY, Moller MB, Tzankov A, Montes-Moreno S, Hu W, Manyam GC, et al. MDM2 phenotypic and genotypic profiling, respective to TP53 genetic status, in diffuse large B-cell lymphoma patients treated with rituximab-CHOP immunochemotherapy: a report from the International DLBCL Rituximab-CHOP Consortium Program. Blood 2013;122:2630–40.
26. Tzankov A, Xu-Monette ZY, Gerhard M, Visco C, Dirnhofer S, Gisin N, et al. Rearrangements of MYC gene facilitate risk stratification in

diffuse large B-cell lymphoma patients treated with rituximab-CHOP. Mod Pathol 2014;27:958–71.
27. Xu-Monette ZY, Wu L, Visco C, Tai YC, Tzankov A, Liu WM, et al. Mutational profile and prognostic significance of TP53 in diffuse large B-cell lymphoma patients treated with R-CHOP: report from an International DLBCL Rituximab-CHOP Consortium Program Study. Blood 2012;120:3986–96.
28. Irizarry RA, Hobbs B, Collin F, Beazer-Barclay YD, Antonellis KJ, Scherf U, et al. Exploration, normalization, and summaries of high density oligonucleotide array probe level data. Biostatistics 2003;4: 249–64.
29. Bolstad BM, Irizarry RA, Astrand M, Speed TP. A comparison of normalization methods for high density oligonucleotide array data based on variance and bias. Bioinformatics 2003;19:185–93.
30. Hu S, Xu-Monette ZY, Tzankov A, Green T, Wu L, Balasubramanyam A, et al. MYC/BCL2 protein coexpression contributes to the inferior survival of activated B-cell subtype of diffuse large B-cell lymphoma and demonstrates high-risk gene expression signatures: a report from The International DLBCL Rituximab-CHOP Consortium Program. Blood 2013;121:4021–31.
31. Kiuchi N, Nakajima K, Ichiba M, Fukada T, Narimatsu M, Mizuno K, et al. STAT3 is required for the gp130-mediated full activation of the c-myc gene. J Exp Med 1999;189:63–73.
32. Fukada T, Hibi M, Yamanaka Y, Takahashi-Tezuka M, Fujitani Y, Yamaguchi T, et al. Two signals are necessary for cell proliferation induced by a cytokine receptor gp130: involvement of STAT3 in anti-apoptosis. Immunity 1996;5:449–60.
33. Joerger AC, Ang HC, Fersht AR. Structural basis for understanding oncogenic p53 mutations and designing rescue drugs. Proc Natl Acad Sci U S A 2006;103:15056–61.
34. Grivennikov SI, Karin M. Dangerous liaisons: STAT3 and NF-kappaB collaboration and crosstalk in cancer. Cytokine Growth Factor Rev 2010;21:11–9.
35. Yu H, Kortylewski M, Pardoll D. Crosstalk between cancer and immune cells: role of STAT3 in the tumour microenvironment. Nat Rev Immunol 2007;7:41–51.
36. Wu K, Chang Q, Lu Y, Qiu P, Chen B, Thakur C, et al. Gefitinib resistance resulted from STAT3-mediated Akt activation in lung cancer cells. Oncotarget 2013;4:2430–8.
37. So JY, Smolarek AK, Salerno DM, Maehr H, Uskokovic M, Liu F, et al. Targeting CD44-STAT3 signaling by Gemini vitamin D analog leads to inhibition of invasion in basal-like breast cancer. PLoS ONE 2013;8: e54020.
38. Liu JL, Wang XY, Huang BX, Zhu F, Zhang RG, Wu G. Expression of CDK5/p35 in resected patients with non–small cell lung cancer: relation to prognosis. Med Oncol 2011;28:673–8.
39. Stewart DA, Bahlis N, Mansoor A. pY-STAT3 and p53 expression predict outcome for poor prognosis diffuse large B-cell lymphoma treated with high dose chemotherapy and autologous stem cell transplantation. Leuk Lymphoma 2009;50:1276–82.
40. Meier C, Hoeller S, Bourgau C, Hirschmann P, Schwaller J, Went P, et al. Recurrent numerical aberrations of JAK2 and deregulation of the JAK2–STAT cascade in lymphomas. Mod Pathol 2009;22: 476–87.
41. Valera A, Lopez-Guillermo A, Cardesa-Salzmann T, Climent F, Gonzalez-Barca E, Mercadal S, et al. MYC protein expression and genetic alterations have prognostic impact in patients with diffuse large B-cell lymphoma treated with immunochemotherapy. Haematologica 2013; 98:1554–62.
42. Barre B, Avril S, Coqueret O. Opposite regulation of myc and p21waf1 transcription by STAT3 proteins. J Biol Chem 2003;278:2990–6.
43. Bowman T, Broome MA, Sinibaldi D, Wharton W, Pledger WJ, Sedivy JM, et al. Stat3-mediated Myc expression is required for Src transformation and PDGF-induced mitogenesis. Proc Natl Acad Sci U S A 2001;98:7319–24.
44. Lee H, Herrmann A, Deng JH, Kujawski M, Niu G, Li Z, et al. Persistently activated Stat3 maintains constitutive NF-kappaB activity in tumors. Cancer Cell 2009;15:283–93.
45. Yang J, Liao X, Agarwal MK, Barnes L, Auron PE, Stark GR. Unphosphorylated STAT3 accumulates in response to IL-6 and activates transcription by binding to NFkappaB. Genes Dev 2007;21:1396–408.
46. Gupta M, Han JJ, Stenson M, Wellik L, Witzig TE. Regulation of STAT3 by histone deacetylase-3 in diffuse large B-cell lymphoma: implications for therapy. Leukemia 2012;26:1356–64.
47. Williams SA, Chen LF, Kwon H, Ruiz-Jarabo CM, Verdin E, Greene WC. NF-kappaB p50 promotes HIV latency through HDAC recruitment and repression of transcriptional initiation. EMBO J 2006;25:139–49.
48. Oki Y, Buglio D, Fanale M, Fayad L, Copeland A, Romaguera J, et al. Phase I study of panobinostat plus everolimus in patients with relapsed or refractory lymphoma. Clin Cancer Res 2013;19:6882–90.
49. Scuto A, Kujawski M, Kowolik C, Krymskaya L, Wang L, Weiss LM, et al. STAT3 inhibition is a therapeutic strategy for ABC-like diffuse large B-cell lymphoma. Cancer Res 2011;71:3182–8.
50. Adida C, Haioun C, Gaulard P, Lepage E, Morel P, Briere J, et al. Prognostic significance of survivin expression in diffuse large B-cell lymphomas. Blood 2000;96:1921–5.